American Mineralogist, Volume 83, pages 569–576, 1998

Single-crystal IR spectroscopy of very strong hydrogen bonds in pectolite, $NaCa_2[Si_3O_8(OH)]$, and serandite, $NaMn_2[Si_3O_8(OH)]$

VERA M.F. HAMMER,[1] EUGEN LIBOWITZKY,[2,3,]* AND GEORGE R. ROSSMAN[3]

[1]Mineralogisch-Petrographische Abteilung, Naturhistorisches Museum Wien, Burgring 7, A-1014 Wien, Austria
[2]Institut für Mineralogie und Kristallographie, Universität Wien-Geozentrum, Althanstrasse 14, A-1090 Wien, Austria
[3]Division of Geological and Planetary Sciences, California Institute of Technology, 170-25, Pasadena, California 91125, U.S.A.

ABSTRACT

Polarized infrared absorption spectra of thin, oriented single-crystal slabs of pectolite and serandite were recorded between 4000 and 350 cm^{-1} at 298 and 83 K. The spectra of both minerals show a broad absorption region parallel to the silicate chains (*b* direction) that is centered around 1000 cm^{-1}, which is interrupted by a transmission window, and which is superimposed by sharp silicate, lattice, and overtone modes. This band is assigned to the OH stretching mode consistent with the alignment of the O-H · · · Ohydrogen bond parallel to *b* and the short O · · · Odistance of 2.45–2.48 Å that was found in previous X-ray structure refinements. At 1396 cm^{-1} (pectolite) and 1386 cm^{-1} (serandite) an OH bending mode is observed in the IR spectra parallel to *c*. At low temperatures, this mode shifts up to higher frequencies (1403 cm^{-1} at 83 K in pectolite), whereas the down-shift of the OH stretching mode cannot be observed due to the extremely broad band width. The slightly higher energy of the bending mode in pectolite indicates a slightly stronger hydrogen bond with respect to serandite. However, the bond length in serandite is slightly shorter than that in pectolite. An asymmetric O-H · · · Obond is confirmed in pectolite and serandite through comparison with different materials with similar, very strong hydrogen bonds and low-energy OH stretching modes.

INTRODUCTION

Pectolite, $NaCa_2[Si_3O_8(OH)]$, and serandite, $NaMn_2[Si_3O_8(OH)]$, occur typically as hydrothermal minerals in cavities and fissures of basic magmatites and as rock-forming minerals in alkaline rocks. An X-ray crystallographic description of pectolite was first given in comparison with monoclinic pyroxenes by Warren and Biscoe (1931). Because of the triclinic structure of pectolite, it was not considered to be a member of the pyroxene group. Peacock (1935) confirmed the triclinic symmetry by numerous morphologic investigations. On the basis of X-ray diffraction patterns, Schaller (1955) found a continuous isostructural series from pectolite to serandite.

The crystal structure of pectolite was first determined by Buerger (1956) and subsequently refined by Prewitt and Buerger (1963). They stated that the most probable location for the H proton is between the undersaturated oxygen atoms O(3) and O(4), which are separated by less than 2.5 Å. A further refinement in the space group $P\bar{1}$ ($Z = 2$) was made by Prewitt (1967) using counter diffractometer data. He proposed that the H proton is associated closer to O(3) leading to an asymmetric O-H · · · O bond. This was also confirmed by an investigation of Takéuchi and Kudoh (1977), who refined a manganoan sample of pectolite. The isotypic structure of serandite was refined by Takéuchi et al. (1976). The H atom position in serandite could not be located exactly, but a residual electron density between O(3) and O(4) was observed.

The crystal structures of both minerals are composed of silicate chains (Si_3O_9 units) running parallel to *b*, which are interconnected by double columns of edge-sharing CaO_6 (resp. MnO_6) octahedra also extending in the *b* direction. The Na atoms have a peculiar, irregular coordination, and connect silicate chains and octahedral columns. The location of the proton between the closely spaced O(3) and O(4) atoms of the silicate chain, induces a very strong hydrogen bond with an O-H vector orientated approximately parallel to the *b* direction (Figs. 1a and 1b). Hence, the silicate unit is best described as $[Si_3O_8(OH)]$. Stacking disorder and polytypism in pectolite and serandite similar to that observed in wollastonite were discussed by Müller (1976).

Because $Z = 2$ and the formulae of pectolite and serandite contain one OH group, the unit cell contains only two OH groups that are symmetrically related by a center of symmetry ($P\bar{1}$). Consequently, only one IR active stretching mode (A_u, asymmetric vibration of the two groups) and one Raman active stretching mode (A_g, symmetric vibration of the groups) is expected (according to the factor group tables by Adams and Newton 1970). If the H sites are fully occupied, the above considerations also exclude the presence of additional OH groups in the structure (except for additional ''impurity'' sites).

* E-mail: eugen.libowitzky@univie.ac.at

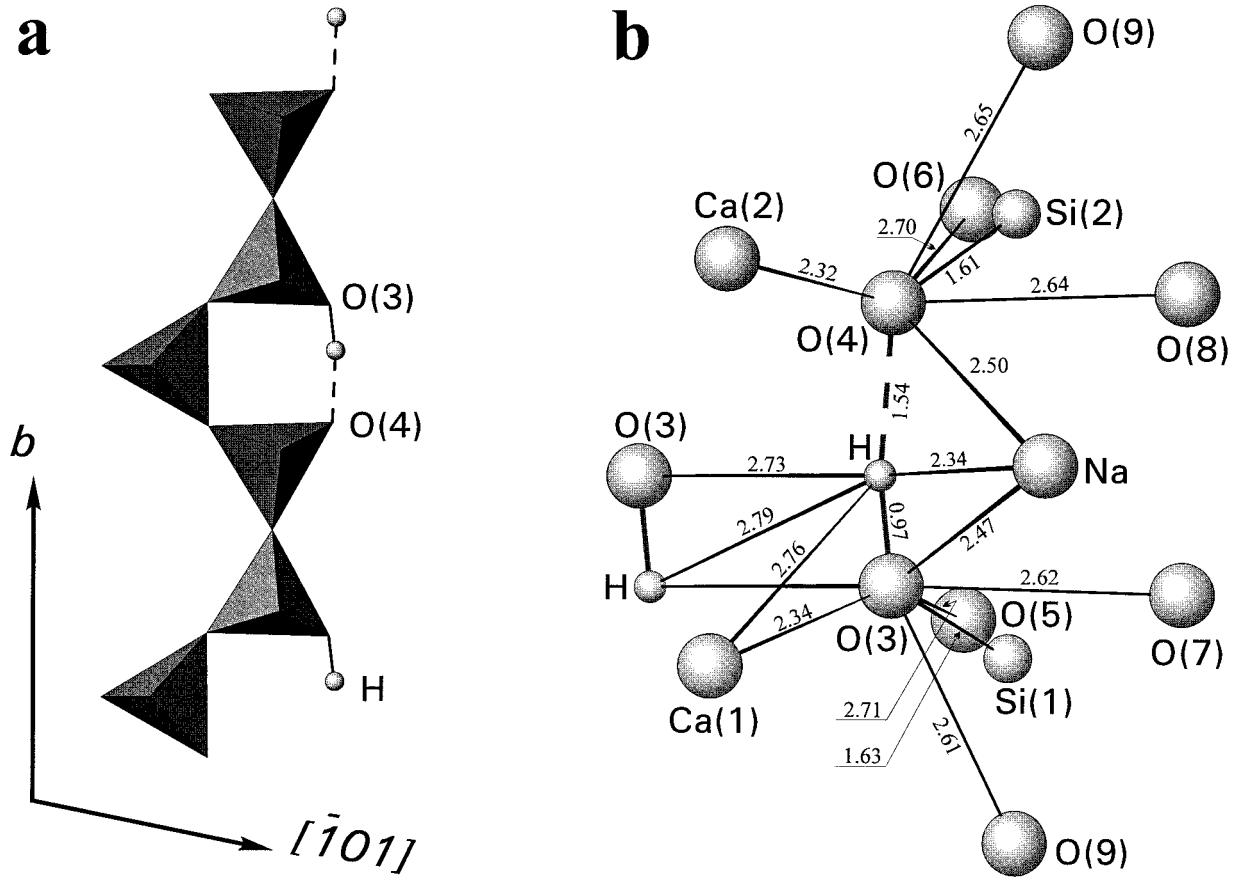

FIGURE 1. (**a**) Schematic drawing of the silicate chain in pectolite and serandite, containing the very strong hydrogen bond between O(3) and O(4). (**b**) The environment of the hydrogen bond showing all interatomic distances (in angstroms) within a sphere of 2.8 Å around O(3), O(4), and H.

This paper is one in a series dealing with spectroscopic features of minerals with very strong hydrogen bonds, e.g., Hammer (1989), Mereiter et al. (1992), Libowitzky (1996), Kohler et al. (1997), Nyfeler et al. (1997), and Beran et al. (1997). The present work characterizes the OH stretching bands of pectolite and serandite and confirms the proposed proton sites and hydrogen bonds with spectroscopic methods. This study also contributes toward understanding the symmetry or asymmetry of very strong hydrogen bonds.

EXPERIMENTAL METHODS

The pectolite samples are from Bergen Hill, New Jersey, and are part of the bulk specimen used by Prewitt (1967). Hence, the composition of the pectolite is close to the end-member, even though FeO and MgO impurities (~1 wt%) are suggested. The serandite samples from Mont St. Hilaire, Quebec, were donated by Michel Picard, Musée de la Nature, Ottawa, sample 75-3. An additional pectolite sample came from the same locality, sample number F89-45. According to Boissonnault and Perrault (1964) the serandite is close to end-member composition. The identity of the material was confirmed by powder X-ray diffraction analysis on a Siemens D5000 diffractometer.

The pectolite samples were oriented according to natural crystal faces and with respect to the perfect cleavage (100) and (001). The serandite samples were oriented with the X-ray precession method. In either case, orientational deviations are considered to be smaller than $\pm 2°$.

Because of the excellent cleavage, the preparation of sufficiently thin crystal slabs was a difficult task. Preliminary investigations showed that slabs with only 50 μm thickness were too thick for the observation of the strong IR absorption bands. Finally, however, unsupported (100) and (001) slabs with only 10 μm thickness, or below, could be prepared with diamond films. A detailed description of the polishing technique is given by Libowitzky and Rossman (1996a) and Nyfeler et al. (1997). The obtained platelets were still too thick to get the silicate modes on scale (this task required sub-micrometer thickness; hence intense silicate modes are truncated in the present spectra), but they proved sufficiently thin for the observation of the OH stretching and bending modes.

Preliminary FTIR measurements were performed on a Perkin Elmer 1760X FTIR spectrometer at the University

Vienna in transmission mode between 5000 and 1000 cm^{-1}, at room temperature, and on oriented, polished single-crystal plates. Even though the thick samples did not facilitate the observation of the strong OH stretching fundamental, they showed overtone and combination bands around 2000, 3000, and 4000 cm^{-1} (see below).

The IR absorption spectra of the final, thin slabs were obtained on a Nicolet 60SX FTIR spectrometer, or, in the case of small sample fragments, on a NicPlan FTIR microscope, both at the California Institute of Technology. The settings with the FTIR spectrometer were: globar source, KBr beamsplitter, gold-wire grid polarizer on AgBr substrate (extinction better than 1:100), DTGS detector, 200 μm sample aperture, 2 cm^{-1} resolution, mean from >256 scans.

The low-temperature spectra were measured in a commercial vacuum cryo-cell with KBr windows (MMR Technologies). A liquid nitrogen oil trap was used after the vacuum pump. Nevertheless, traces of organic impurities from the vacuum oil could not be avoided completely in the low-temperature spectra. Different settings for the FTIR microscope were: mirror objective (Cassegrain) 15× / 0.58 N.A., MCT detector (LN_2-cooled), 50 × 200 μm sample aperture, 4 cm^{-1} resolution, mean from 1024 scans. Even though dual knife-edge apertures were used (i.e., identical rectangular apertures below and above the sample), light leakage caused the microscope spectra to be truncated above $A = 2.4$. The polarizer was mounted below the sample in the object stage of the microscope to minimize polarization mixing by the convergent beam of light. In all cases the polarizer was kept constant, whereas the sample was rotated according to the desired orientation.

Several deuteration experiments on serandite and pectolite were performed, but failed for the following reasons: (1) Preliminary experiments with pectolite powder in D_2O at low temperatures (≤100 °C) and ambient pressure resulted in only minor D substitution (R.D. Aines, personal communication). The IR powder spectra did not indicate any OH or OD stretching bands (this is common in IR powder spectra of materials with very strong hydrogen bonds; see discussion below). (2) Preliminary deuteration experiments with 50 to 100 μm thick pectolite crystals (unpolished) at 250 °C in a Parr vessel resulted in surface alteration of the crystals. (3) A 14 d deuteration experiment with a polished, 10 μm thick platelet of serandite at 250 °C in a Parr vessel resulted in oxidation of Mn^{2+} to Mn^{4+} (indicated by the black, opaque color of the resulting slab). (4) A final 15 week experiment with an oriented, polished, 6 μm thick pectolite platelet at 250 °C in a Parr autoclave resulted in the decomposition of the material. Thus, it seems that pectolite and serandite are thermodynamically stable only at very low-thermal conditions, or that D substitution in the minerals shifts the stability limits into *P-T* regions outside the applied deuteration conditions.

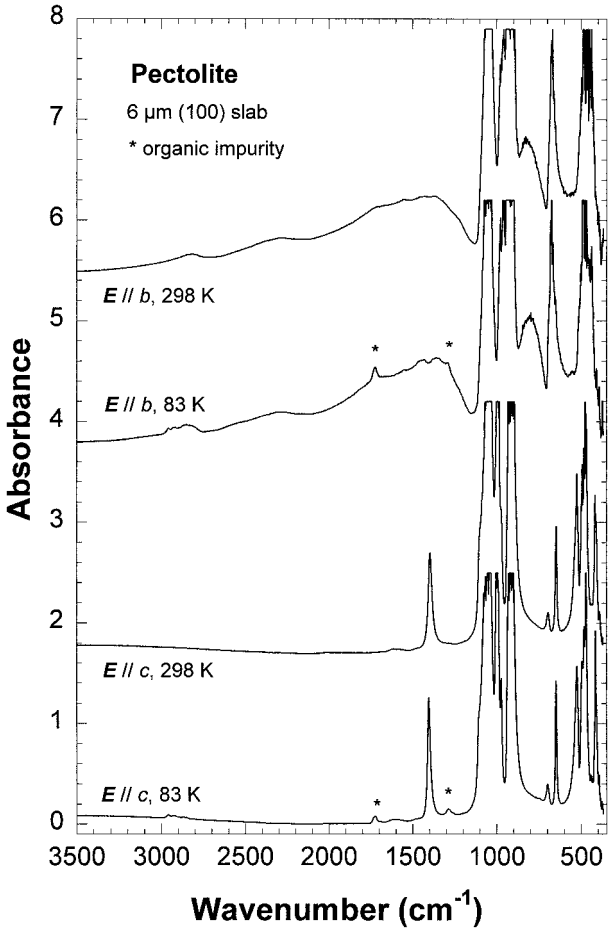

FIGURE 2. Polarized FTIR absorption spectra of pectolite at low and ambient temperatures. Spectra are vertically offset by $A = 1.7$, 2.0, and 1.7 each. Readability was improved by removing excessive noise above $A = 2.5$.

RESULTS

Polarized IR absorption spectra of pectolite are presented in Figure 2, those of serandite are shown in Figures 3 and 4. In general, the spectra of pectolite (**E** ∥ *b* and **E** ∥ *c*) and serandite (**E** ∥ *b* and **E** ∥ *c*) are very similar (as might be expected from the isotypic structures).

The **E** ∥ *a* spectrum of serandite (and by analogy, pectolite) is generally flat in the region between 4000 and 1200 cm^{-1}, except for very shallow, wavy features that (by comparison with other thin samples) are spaced in accordance with the respective thickness of the slabs, suggesting that these are interference fringes in the extremely thin, doubly polished platelets. Around 1200–800 cm^{-1} the stretching modes of the silicate tetrahedra are observed (truncated), and the silicate bending modes and the lattice modes of the remaining structural constituents occur at lower energies (Farmer 1974).

The **E** ∥ *b* spectra of both minerals show a very broad, absorbing region, which starts from around 3500 cm^{-1} and increases to a preliminary maximum around 1500–

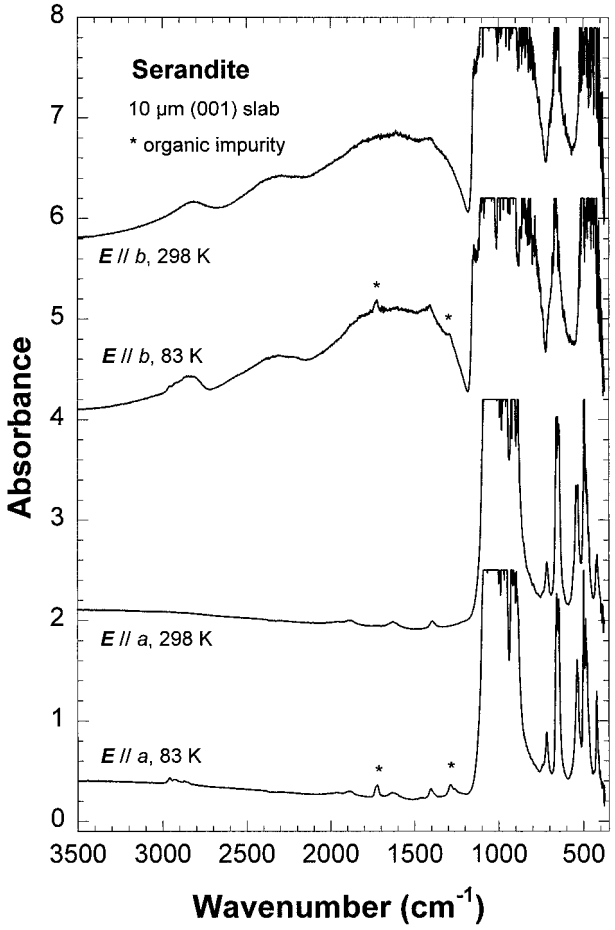

FIGURE 3. Polarized FTIR absorption spectra of serandite at low and ambient temperatures. Spectra are vertically offset and improved as in Figure 2.

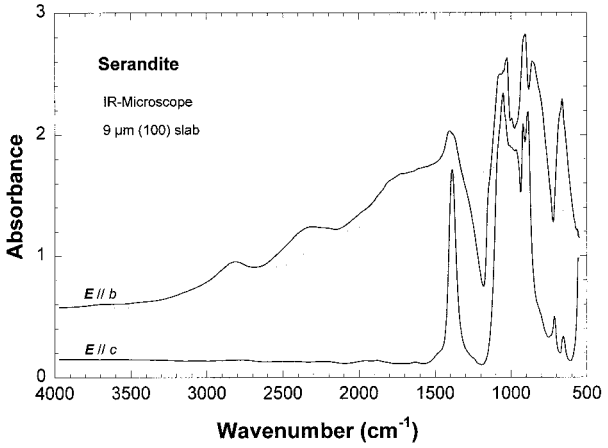

FIGURE 4. Polarized FTIR microscope absorption spectra of serandite. The **E** ∥ *b* spectrum is vertically offset by $A = 0.5$. Silicate stretching modes between 800 and 1200 cm^{-1} are truncated above $A = 2.4$. The bold gray curve indicates the suggested shape of the broad, low-energy OH stretching band in the **E** ∥ *b* spectrum.

1400 cm^{-1}. At a first glance, this part of the spectrum resembles an elevated and tilted background line. A typical feature of this line are also the shallow humps around 2800, 2300, and 1750 cm^{-1} that are definitely not caused by interference fringes. The region of increasing absorbance is suddenly interrupted by an asymmetric gap around 1200 cm^{-1}. Similar to the **E** ∥ *a* spectra, the silicate stretching modes appear around 1200–800 cm^{-1} (truncated) and the silicate bending and lattice modes below 800 cm^{-1}. However, it is important to note that the background line between the strong and sharp silicate and lattice modes (i.e., the baseline between the peaks) is still elevated, which is quite different to the behavior in the **E** ∥ *a* and **E** ∥ *c* spectra. The **E** ∥ *a* and **E** ∥ *c* spectra indicate further that there are no general background problems; both show a flat baseline in all samples both in the microscope and in the usual sample compartment of the spectrometer. It is evident that the **E** ∥ *b* spectra, which probe the absorption parallel to the silicate chains and parallel to the O-H vector direction, must contain the OH stretching mode (assuming that previous crystal structure investigations are correct). As a consequence, only the broad, intense absorbing region, which shows up as a unique feature in the **E** ∥ *b* spectra, can be correlated with the stretching vibration of the very strong hydrogen bond. The shape and position of this broad band absorption are in excellent agreement with spectra of various organic and inorganic compounds with similar, very strong hydrogen bonds, as discussed below.

The **E** ∥ *c* spectra are similar to the **E** ∥ *a* spectra except that they show an additional mode at 1396 cm^{-1} (pectolite) and 1386 cm^{-1} (serandite). This sharp band is assigned to a bending mode of the strongly hydrogen-bonded OH group, which is also confirmed by the polarization direction of the band perpendicular to the O-H vector direction. This assignment was also proposed previously from powder spectra by Ryall and Threadgold (1966) even though they could not find the related OH stretching band. An assignment of the sharp peak to an OH stretching mode is not reasonable, because sharp OH stretching modes are only known in the region above ~3000 cm^{-1}, whereas OH stretching modes around 1400 cm^{-1} are extremely broad (e.g., Nyfeler et al. 1997). The question, why the preferred bending motion is only active in the *c* direction and not parallel to *a*, cannot be answered conclusively. A possible reason may be that the OH bending mode parallel to *c* vibrates almost perpendicular to the Na-H-O(3) line, which seems more reasonable than a bending motion parallel to this line (~∥ *a*) moving the H atom closer to the Na atom (Fig. 1b).

Another OH bending mode might be assumed in the **E** ∥ *b* spectra between 850 and 800 cm^{-1} adjacent to the silicate stretching modes. Nevertheless, this bending mode cannot be reconciled with the direction of the very strong hydrogen bond in the structure, hence it had to be assigned to an additional OH site in the structure. Ac-

cording to Novak (1974), the energy of this mode is in agreement with a weak hydrogen bond, thus the stretching band should be expected in the 3500 to 3000 cm^{-1} wavenumber region. However, a stretching band in the **E** ∥ *a* or **E** ∥ *c* spectra, indicating a weak hydrogen bond, is not observed. The band between 850 and 800 cm^{-1} may be also explained by another silicate stretching mode that is active only in the *b* direction.

At low temperatures the spectra are similar to those at room-temperature. As usual, the bands become slightly sharper and more intense (peak height), but due to the broad band absorption in the **E** ∥ *b* spectra, a quantitative band shift cannot be observed. Only a weak increase in the energy of the OH bending mode in pectolite from 1396 cm^{-1} (at 298 K) to 1403 cm^{-1} (at 83 K) is quantitatively visible in the **E** ∥ *c* spectra. In a similar way, spectroscopic differences between pectolite and serandite are mainly characterized by a different energy of the OH bending mode and the various combination and overtone bands, whereas differences in the broad band OH stretching vibration in the **E** ∥ *b* spectra cannot be observed.

Bands observed in unpolarized spectra of thick (010) crystal slabs occur around 1850, 2790, and 3950 cm^{-1} in serandite, and around 1950, 2850, and 3980 cm^{-1} in pectolite probably represent overtone or combination bands of the silicate and the OH stretching modes. However, because the silicate stretching vibrations and the center of the broad OH stretching band occur at similar energies, these bands cannot be assigned unambiguously. The differences in the band energies between the modes of serandite and those of pectolite (pectolite > serandite) suggest however, that the OH stretching mode is involved in these non-fundamental modes. The fact that the observed bands show lower wavenumbers than expected from a simple multiplication or addition is well explained by (and an additional argument for) the strong anharmonicity of short and very strong hydrogen bonds (see below).

Another explanation for the above mentioned bands as well as for the shallow humps around 1750, 2300, and 2800 cm^{-1} in the polarized **E** ∥ *b* spectra (Figs. 2–4) may be additional OH groups in the structure. According to the low wavenumbers between 2800 and 1750 cm^{-1} these bands must be assigned to moderately strong hydrogen bonds. However, the required short O · · · O distances cannot be observed in the structure. Only the distances between the coordinating O atoms of the SiO_4 tetrahedra show distances between 2.6 and 2.7 Å. However, the incorporation of H atoms into SiO_4 tetrahedra would require Si vacancies, which, in turn would increase the size of the polyhedron, and finally result in weak hydrogen bonds and high-energetic OH stretching bands (e.g., the hydro-grossular $(OH)_4$ substitution shows bands around 3650 cm^{-1}). As discussed below, the observed wavy features are resonance phenomoena of the broad OH stretching band in the **E** ∥ *b* spectra and overtones of various low-energetic IR modes (e.g., silicate stretching modes).

IR SPECTROSCOPIC FEATURES OF VERY STRONG HYDROGEN BONDS

The strength (and length) of an O-H · · · O hydrogen bond is conveniently expressed by the distance between the donor and acceptor O atoms ($R_{O \cdots O}$). A distance larger than 2.7 Å is considered a weak hydrogen bond, a separation by 2.5–2.7 Å characterizes a strong hydrogen bond, and a distance below 2.5 Å (down to ~2.39 Å at ambient conditions) defines a very strong hydrogen bond (Emsley et al. 1981). The IR stretching bands (ν) of the hydrogen bonded O-H units usually occur at 3700–3200 cm^{-1} (weak hydrogen bonds), 3200–1600 cm^{-1} (strong hydrogen bonds), and 1600–600 cm^{-1} (very strong hydrogen bonds). Thus, the correlation between $R_{O \cdots O}$ and stretching frequency (based upon attenuation of the O-H force constant with increasing strength of the H · · · O bond) is used to classify and characterize hydrogen bonds (Novak 1974).

Strong and very strong hydrogen bonds are not only characterized by a decreasing wavenumber, but also by an increasing band width and an increasing integrated intensity of the OH stretching band (Hadzi and Bratos 1976). The former is caused by repeated combination of the stretching mode (ν) with the very low-frequent breathing mode (σ) of the hydrogen bond, the latter is a function of the attenuated principal O-H bond (by increasing the O · · · H bond strength) that facilitates easier IR excitation. Moreover, the potential energy surface of the O-H · · · O bond changes with increasing hydrogen bond strength from an asymmetric single minimum type (weak hydrogen bond) via an asymmetric double minimum type via a symmetric double minimum type with low energy barrier to a symmetric single minimum type at an O · · · O distance below 2.42 Å (Emsley et al. 1981). As a consequence, hydrogen bonds show an increasing anharmonicity (Sandorfy 1976) with increasing hydrogen bond strength (except for the symmetric single minimum type). The strong anharmonicity of the broad band causes peculiar features like anomalous deuteration shifts (ν_{OH}/ν_{OD} close to 1.0, instead of 1.35 for weak hydrogen bonds), observation of IR absorption bands that are actually forbidden by normal mode analysis, and finally different resonance phenomena. The latter are observed in these spectra in the form of (1) enhanced combination and overtones, if they fall in the region of the broad OH stretching absorption, and (2) gaps within the broad absorption band that have been described as (and partially explained by) ''Fermi resonance,'' ''Evans type transmission windows,'' or ''Evans holes,'' ''anharmonicity resonance'' (Hadzi and Bratos 1976), or most recently ''antiresonance'' and ''Fano type'' features (Struzhkin et al. 1997). The peculiar shape of these features caused by resonance of the broad band OH absorption with interfering bands was even confirmed by theoretical calculations (Hadzi and Bratos 1976).

Examples for IR spectra of very strong hydrogen bonds have been published in the past decades in numerous pa-

pers of the chemical literature. For a compilation of some of them and for more general aspects of these spectra, the reader is referred to Hadzi (1965), Novak (1974), and Hadzi and Bratos (1976). Typical spectra of materials with very strong hydrogen bonds, with a band maximum between 1500 to 500 cm^{-1} and overlapping gaps (''transmission windows'') and interfering bands, have been called ''Hadzi type ii spectra'' (Hadzi 1965) and substances in which they occur have been called Speakman-Hadzi compounds (Kreevoy et al. 1998).

Moreover, examples of polarized IR absorption spectra of minerals with short or very short hydrogen bonds have been recently published by Libowitzky (1996), Daniels et al. (1997), Kohler et al. (1997), Nyfeler et al. (1997), and Beran et al. (1997). The common feature of these polarized spectra of very strong hydrogen bonds is that they show the broad band shape and the resonance phenomena described above, and that they yield the broad band IR absorption in the correct polarization direction, i.e., parallel to the O-H vector direction in the crystal structure.

Discussion

Considering IR spectroscopic features of very strong hydrogen bonds (reviewed above), the spectra parallel to the *b* direction (Figs. 2–4) can be interpreted conclusively. The broad band absorption does not end abruptly at the gap (the transmission window) at 1200 cm^{-1}, but it continues after the gap in the 1000–350 cm^{-1} wavenumber region (which was described as elevated baseline in the Results section). Thus, the two broad absorption regions below and above the 1200 cm^{-1} gap belong to a single, extremely broad OH stretching band, which extends from 3500 cm^{-1} into the region below 350 cm^{-1}. This broad band, which is indicated in Figure 4, is interrupted by a transmission window at 1200 cm^{-1} resulting from the resonance of the sharp silicate modes with the anharmonic OH stretching vibration. As a consequence, the center of the band is not observed around 1400 cm^{-1} but rather around 1000 cm^{-1}, where it is corrupted by the silicate stretching modes.

Using the diagrams of Novak (1974) that correlate the OH stretching energies with O-H · · · O bond lengths (positive correlation), good agreement between the hydrogen bond distances from previous structure refinements (e.g., Takéuchi et al. 1976) and the present spectroscopic results is obtained. The short O-H · · · O distances of 2.48 Å (pectolite) and 2.45 Å (serandite) correlate well with the observed OH stretching band energy of ~1000 cm^{-1}. (The expected O-H · · · O distance is around 2.46–2.47 Å.) This correlation is only approximate, because the energy of the smooth, broad band cannot be determined with higher accuracy, and more accurate structural data were not available at that time.

The correlation diagram of Nakamoto et al. (1955) shows unsatisfactory agreement, because the expected stretching bands appear at too high energies. It is our experience that this diagram cannot be used for very strong hydrogen bonds (the respective frequencies are not even contained), and the correlating wavenumbers appeared too high even for weak hydrogen bonds in previous investigations. Unfortunately, the most recent and accurate correlation diagrams (even though better defined by neutron structure data and isotopically dilute systems, e.g., Mikenda 1986) cannot be used, because they cover only the range of weak to moderately strong hydrogen bonds.

Using another correlation diagram (Novak 1974) that relates OH stretching and out-of-plane bending energies (negative correlation), weak agreement between the observed mode around 1000 cm^{-1} and that at ~1390 cm^{-1} is obtained. According to Novak, the expected out-of-plane bending mode should occur at approximately 1250 cm^{-1}. However, there is no evidence that the observed bending mode in pectolite and serandite actually belongs to the out-of-plane bending instead of the in-plane bending, and, in addition, the observed mode may be a combination of the bending and some low-energy band. Nevertheless, both above mentioned correlations and the OH bending energies of pectolite and serandite suggest that the hydrogen bond in serandite is slightly weaker (longer) than that in pectolite, whereas crystal structure refinements indicate a slightly weaker (longer) bond in pectolite (e.g., Takéuchi et al. 1976). However, cationic effects on the respective vibrational modes, which may be considerably different in pectolite (Ca^{2+}) and serandite (Mn^{2+}), are not considered by these correlations.

The temperature-dependent band shifts are in agreement with the usual behavior of hydrogen-bonded OH groups (Lutz 1995). Due to the low-temperature contraction of the structure the hydrogen bond lengths decrease too. Thus, the low-temperature stretching mode occurs at lower energies (quantitatively not visible, as mentioned above) and the low-temperature bending mode at the observed higher energies.

The intensity of the broad OH stretching band at ~1000 cm^{-1} provides an additional argument that it is correctly assigned. The intensity of the band in pectolite is in agreement (±10%) with the predicted band intensity based on the recent calibration of Libowitzky and Rossman (1997) obtained with stoichiometric mineral hydrates and hydroxides. Furthermore, the trend of Paterson (1982), which correlates band energies of OH stretching bands in quartz and glasses with integrated molar absorption coefficients, predicts a calculated intensity in pectolite in agreement (±10%) with the experimental data (even though the range of Paterson's diagram is severely exceeded).

Two questions deserve further discussion: (1) Why has the OH stretching mode of pectolite and serandite never been observed before? (2) Is there any conclusive spectroscopic evidence for the symmetry or asymmetry of such a short hydrogen bond?

(1) Previous investigations and spectroscopic recordings (e.g., Ryall and Threadgold 1966; Angela 1972; Hammer 1989) only used pectolite powder in the form of KBr pellets or single-crystals that were too thick for the

observation of the strong band. Because the broad OH stretching band is only visible in one polarization direction (**E** ∥ *b*), its intensity is attenuated disproportionally in a powder sample (due to the logarithmic relation between transmission and absorbance; see Libowitzky and Rossman 1996b). Even if the band were visible it could not be distinguished from a smoothly increasing background in the powder sample. This was also shown in other minerals with very strong hydrogen bonds, e.g., mozartite (Nyfeler et al. 1997) and the natrochalcite group (Beran et al. 1997).

(2) Comparison of spectroscopic features among other materials with very short hydrogen bonds yields arguments for an asymmetric O-H · · · O bond. Novak (1974) shows the absorption spectrum of potassium hydrogen diacetate that has a similar O-H · · · O distance of 2.48 Å. The broad OH stretching absorption is similar to the spectra of pectolite and serandite (even if the center of the broad band occurs at somewhat higher energies), the bending mode is not assigned. In mozartite (Nyfeler et al. 1997), a similar IR spectrum and a similar O-H · · · O distance were observed, and IR spectra of minerals of the natrochalcite series (where asymmetric hydrogen bonds have been found by neutron diffraction) also resemble those of the present study.

Structural investigations indicate that very strong hydrogen bonds with $R_{O \cdots O}$ = 2.45–2.48 Å are generally asymmetric. The correlation diagram between O · · · O and O-H distances (Franks 1973) shows that only at an O · · · O distance of ~2.42 Å the O-H distance is ~1.20 Å, which means a symmetrical bond. In addition, IR stretching vibrations of very short and symmetric hydrogen bonds are observed below 1000 cm^{-1} and do not show extremely broad band shapes because of reduced anharmonicity in a symmetric potential (cf. spectra in Novak 1974). Thus, we suggest that the hydrogen bonds in pectolite and serandite are asymmetric.

Acknowledgments

We thank C.T. Prewitt and M. Picard, Musée Canadien de la Nature, Ottawa, for the serandite and pectolite samples. Precession photographs were performed at the ETH Zürich. Preliminary IR measurements on pectolite were performed by R.D. Aines, Caltech. Editor A.M. Hofmeister and Associate Editor H. Keppler helped to improve the presentation and the transparency of the manuscript. E.L. is indebted to the Fonds zur Förderung der wissenschaftlichen Forschung, Austria for financial support during an Erwin-Schrödinger fellowship, project J01098-GEO, at the California Institute of Technology. G.R.R. acknowledges financial support from the National Science Foundation, grant EAR-9218980.

References cited

Adams, D.M. and Newton, D.C. (1970) Tables for factor group and point group analysis. Beckman-RIIC Ltd., London.

Angela, M.F. (1972) Sulla pectolite di Saint Vincent (Valle d'Aosta). Periodico di Mineralogia, 41, 281–289.

Beran, A., Libowitzky, E., and Giester, G. (1997) The hydrogen bond system in natrochalcite-type compounds-an FTIR spectroscopic study of the $H_3O_2^-$ unit. Mineralogy and Petrology, 61, 223–235.

Boissonnault, J. and Perrault, G. (1964) Serandite from St. Hilaire, Quebec. Canadian Mineralogist, 8, 132.

Buerger, M.J. (1956) The determination of the crystal structure of pectolite. Zeitschrift für Kristallographie, 108, 248–262.

Daniels, P., Krosse, S., Werding, G., and Schreyer, W. (1997) Pseudosinhalite, a new hydrous MgAl-borate: synthesis, phase characterization, crystal structure, and *PT*-stability. Contributions to Mineralogy and Petrology, 128, 261–271.

Emsley, J. (1981) Very strong hydrogen bonding. Chemical Society Reviews, 9, 91–124.

Farmer, V.C., Ed. (1974) The Infrared Spectra of Minerals, 539 p. Mineralogical Society, London.

Franks, F., Ed. (1973) Water: A Comprehensive Treatise, vol. 2, 684 p. Plenum, New York.

Hadzi, D. (1965) Infrared spectra of strongly hydrogen-bonded systems. Pure and Applied Chemistry, 11, 435–453.

Hadzi, D. and Bratos, S. (1976) Vibrational spectroscopy of the hydrogen bond. In P. Schuster, G. Zundel, and C. Sandorfy, Eds., The Hydrogen Bond—Recent Developments in Theory and Experiments, p. 565–611. North-Holland Publishing Company, Amsterdam.

Hammer, V.M.F. (1989) IR-spektroskopische quantitative OH-Bestimmung an Rutil und Titanit aus verschiedenen Paragenesen. Das Problem des Auftretens von OH-Streckschwingungen bei extrem kurzen O-H-O Bindungslängen am Beispiel des Pektoliths. Ph.D. thesis, University Vienna, Austria.

Kohler, T., Armbruster, T., and Libowitzky, E. (1997) Hydrogen bonding and Jahn-Teller distortion in groutite, α-MnOOH, and manganite, γ-MnOOH, and their relations to the manganese dioxides ramsdellite and pyrolusite. Journal of Solid State Chemistry, 133, 486–500.

Kreevoy, M.M., Marimanikkuppam, S., Young, V.G., Baran, J., Schultz, A., and Trouw, F. (1998) The proton potential function and dynamics in sodium bis(4-nitrophenoxide) dihydrate. Berichte der Bunsengesellschaft für Physikalische Chemie, 102, in press.

Libowitzky, E. (1996) Single-crystal IR spectroscopy of MeO(OH) minerals (Me = Al, Fe, Mn). Mitteilungen der Österreichischen Mineralogischen Gesellschaft, 141, 134–135.

Libowitzky, E. and Rossman, G.R. (1996a) FTIR spectroscopy of lawsonite between 82 and 325 K. American Mineralogist, 81, 1080–1091.

——— (1996b) Principles of quantitative absorbance measurements in anisotropic crystals. Physics and Chemistry of Minerals, 23, 319–327.

——— (1997) An IR absorption calibration for water in minerals. American Mineralogist, 82, 1111–1115.

Lutz, H.D. (1995) Hydroxide ions in condensed materials—correlation of spectroscopic and structural data. Structure and Bonding, 82, 85–103.

Mereiter, K., Zemann, J., and Hewat, A.W. (1992) Eglestonite, $[Hg_2]_3Cl_3O_2H$: Confirmation of the chemical formula by neutron powder diffraction. American Mineralogist, 77, 839–842.

Mikenda, W. (1986) Stretching frequency versus bond distance correlation of O-D(H) · · · Y (Y = N, O, S, Se, Cl, Br, I) hydrogen bonds in solid hydrates. Journal of Molecular Structure, 147, 1–15.

Müller, W.F. (1976) On stacking disorder and polytypism in pectolite and serandite. Zeitschrift für Kristallographie, 144, 401–408.

Nakamoto, K., Margoshes M., and Rundle, R.E. (1955) Stretching frequencies as a function of distances in hydrogen bonds. Journal of the American Chemical Society, 77, 6480–6486.

Novak, A. (1974) Hydrogen bonding in solids. Correlation of spectroscopic and crystallographic data. Structure and Bonding, 18, 177–216.

Nyfeler, D., Hoffmann, C., Armbruster, T., Kunz, M., and Libowitzky, E. (1997) Orthorhombic Jahn-Teller distortion and Si-OH in mozartite, $CaMn^{3+}O[SiO_3OH]$: a single-crystal X-ray, FTIR, and structure modeling study. American Mineralogist, 82, 841–848.

Paterson, M.S. (1982) The determination of hydroxyl by infrared absorption in quartz, silicate glasses and similar materials. Bulletin de Minéralogie, 105, 20–29.

Peacock, M.A. (1935) On pectolite. Zeitschrift für Kristallographie, 90, 97–111.

Prewitt, C.T. (1967) Refinement of the structure of pectolite, $Ca_2NaHSi_3O_9$. Zeitschrift für Kristallographie, 125, 298–316.

Prewitt, C.T. and Buerger, M.J. (1963) Comparison of the crystal structures of wollastonite and pectolite. Mineralogical Society of America Special Paper, 1, 293–302.

Ryall, W.R. and Threadgold, I.M. (1966) Evidence for $[(SiO_3)_5]_\infty$ type

chains in inesite as shown by X-ray and infrared absorption studies. American Mineralogist, 51, 754–761.

Sandorfy, C. (1976) Anharmonicity and hydrogen bonding. In P. Schuster, G. Zundel, and C. Sandorfy, Eds., The Hydrogen Bond—Recent Developments in Theory and Experiments, p. 613–654. North-Holland Publishing Company, Amsterdam.

Schaller, W.T. (1955) The pectolite-schizolite-serandite series. American Mineralogist, 40, 1022–1031.

Struzhkin, V.V., Goncharov, A.F., Hemley, R.J., and Mao, H. (1997) Cascading Fermi resonances and the soft mode in dense ice. Physical Review Letters, 78, 4446–4449.

Takéuchi, Y. and Kudoh, Y. (1977) Hydrogen bonding and cation ordering in Magnet Cove pectolite. Zeitschrift für Kristallographie, 146, 281–292.

Takéuchi, Y., Kudoh, Y., and Yamanaka, T. (1976) Crystal chemistry of the serandite-pectolite series and related minerals. American Mineralogist, 61, 229–237.

Warren, B.E. and Biscoe, J. (1931) The crystal structure of the monoclinic pyroxenes. Zeitschrift für Kristallographie, 80, 391–401.

Manuscript received March 20, 1997
Manuscript accepted December 10, 1997
Paper handled by Hans Keppler